CERN-ACC-NOTE-2019-0023

2019.06.17

marco.d'andrea@cern.ch

Operational Aspects of Crystal Collimation with Proton Beams

M. D'Andrea, D. Mirarchi, S. Redaelli, B. Salvachua Ferrando, L. Nevay, R. Rossi, W. Scandale, S. Montesano, F. Galluccio, P. Serrano Galvez, C. Dionisio Barreto, M. Butcher, I. Lamas Garcia
CERN, Geneva, Switzerland

Keywords: LHC, collimation, crystal, UA9

Summary

During MD4167, performed on September 12$^{\text{th}}$ 2018, silicon crystals for a crystal-assisted collimation system were tested, with particular focus on operational aspects such as evaluation of cleaning performances and deployment during dynamical phases of the machine. Crystal collimation is studied as an alternative scheme for ion collimation at the HL-LHC. Tests with proton beams are fundamental to perform the initial setup of the system in preparation of the ion run 2018.

1 Introduction

The crystal collimation concept relies on the usage of bent crystals that can deflect halo particles at large angles of up to tens of μrad, as opposed to the standard LHC multi-stage collimation where an amorphous primary collimator scatters halo particles at a few μrad onto several secondary collimators. Crystal primaries could in principle send halo particles coherently onto a single absorber. A setup that uses only existing secondary collimators as absorbers for the channeled beam has been conceived for crystal collimation beam tests in IR7 [1]. Between 2015 and 2018, four bent crystals were installed in IR7, one for each cleaning plane on both Beam 1 and Beam 2. During the years, these crystals were tested and channeling was successfully observed at injection and top energy for both proton and ion beams. The main goal of this MD was to assess operational aspects of crystal-assisted collimation, such as evaluate its cleaning performances with respect to the standard system and verify if the crystals can be kept in channeling conditions during dynamical phases of the machine, e.g. the energy ramp. First tests were performed in 2016, during which the horizontal crystal on Beam 1 was successfully kept in channeling during the ramp [2, 3]. This MD marks the first attempt at keeping all four crystals in channeling conditions

during the ramp at the same time. First preliminary measurements to characterize the crystal devices were performed during the first MD blocks but were affected by a number of issues that limited the machine availability [4]. During this third MD the characterization was completed including more loss maps, and a full energy ramp with all four crystals in channeling conditions at the same time was attempted.

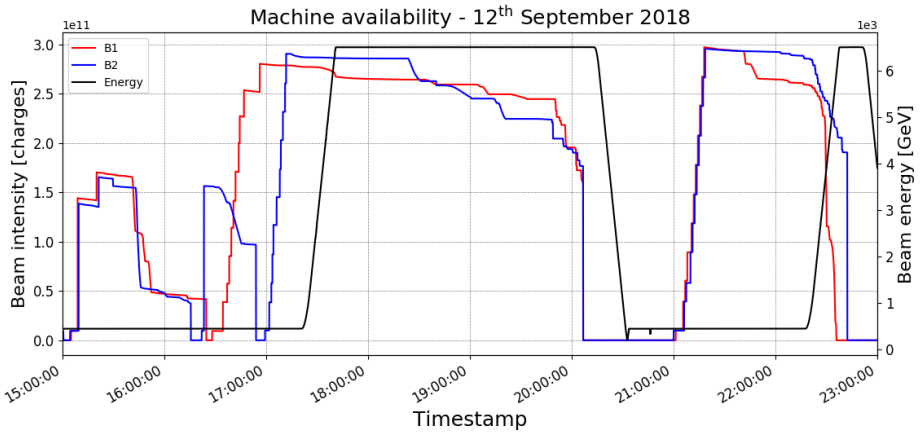

Figure 1: Beam 1 and Beam 2 intensity and energy during the MD.

2 Beam Setup

The MD was performed using several low-intensity bunches at both injection and flat top energy with standard 2018 optics for both Beam 1 and Beam 2, in a configuration that was extensively tested in previous crystal MDs [3, 5–8]. The transverse dumper (ADT) was used to excite the beam with white noise, as in standard collimation loss maps, to achieve controlled primary beam losses on crystals and/or collimators. To have enough losses for the time needed to complete measurements such as angular scans, the ADT window was enlarged to act on three different bunches. This allows to achieve sufficiently high loss rates for longer times. For this reason, the filling scheme consisted of 3-pilot trains with 2 μs spacing between each train and 3 μs spacing between each bunch. For machine protection reasons, up to 30 bunches with total intensity below $3 \cdot 10^{11}$ protons are allowed at flat top. At injection nominal bunches can be used respecting the limit of $5 \cdot 10^{11}$ protons. The energy ramp is performed following the same procedure established in previous tests [2]. Ramp functions for both the linear and angular stage of each crystal are generated with the same model used for standard collimators. The beginning and ending point are fixed to the position and orientation previously found during the alignment and the angular scans respectively. Several low intensity bunches are individually excited during the ramp to verify if channeling conditions are kept.

The scheduled measurements involved the following main activities:

1. beam-based alignment of the crystal with respect to the beam orbit and transverse positioning as primary collimator;

2. angular scan to find the optimal channeling condition;
3. transverse scan of the channeled beam with a secondary collimator;
4. cleaning measurements through loss maps with the crystal in channeling position;
5. ramp function generation for all crystals and for both the rotational and linear stage;
6. energy ramp with crystals as primary collimators in channeling orientation and loss maps measured at different energies.

Fig. 1 shows the intensity and energy of the beams during the MD, which allowed to carry out the full program up until the energy ramp with crystals. Reliable measurements after the ramp midpoint were impossible due to a trip of several power converters of orbit correctors.

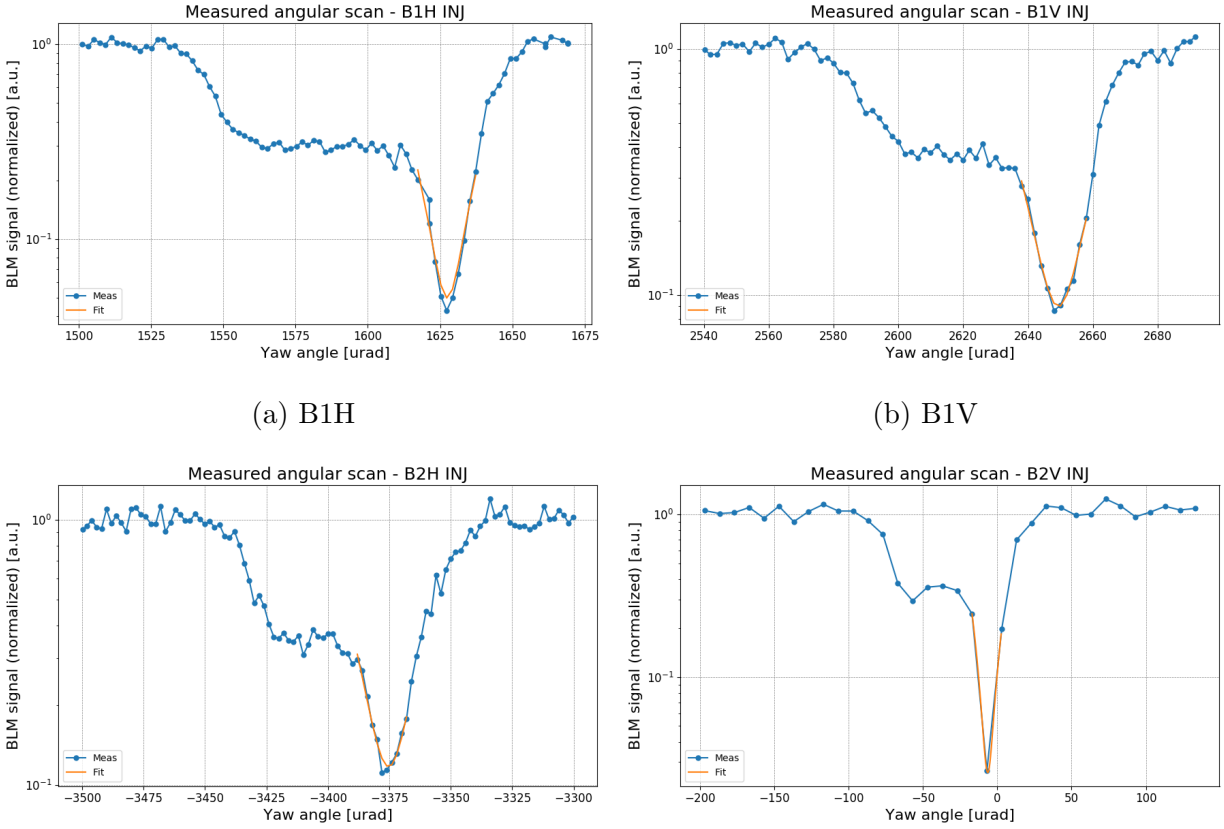

(a) B1H

(b) B1V

(c) B2H

(d) B2V

Figure 2: Angular scans at injection energy. The BLM signal has been normalized to the particle flux and to the amorphous level.

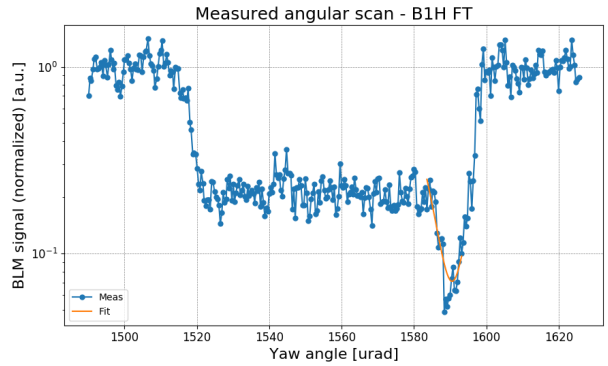

(a) B1H

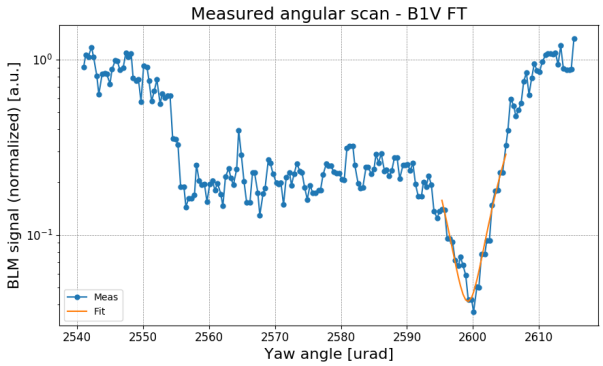

(b) B1V

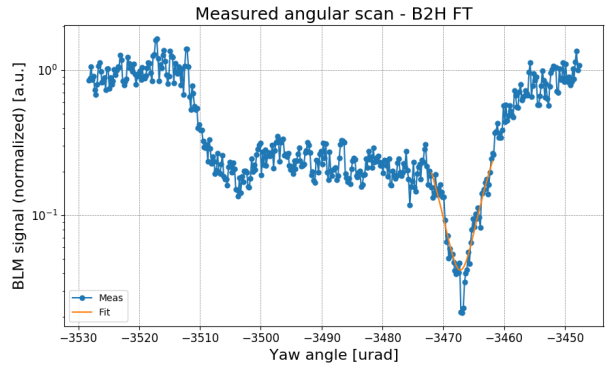

(c) B2H

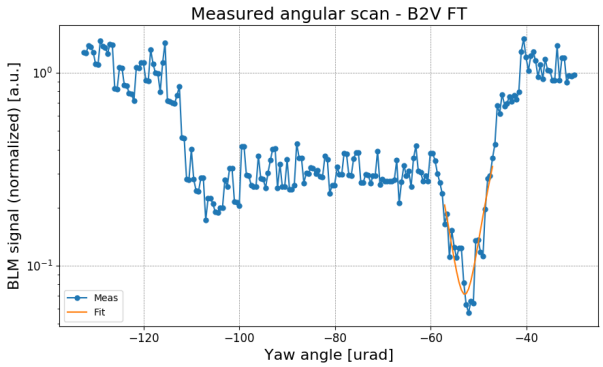

(d) B2V

Figure 3: Angular scans at flat top energy. The BLM signal has been normalized to the particle flux and to the amorphous level.

	Reduction factor		**Optimal channeling orientation [μrad]**		**Bending angle [μrad]**	**Multiturn CH efficiency**
	Inj	**FT**	**Inj**	**FT**	**FT**	**FT**
B1H	20.1	14.1	1627.3	1590.4	not performed	not performed
B1V	11.1	24.0	2650.0	2599.3	38.1	∼74%
B2H	8.5	23.8	-3376.0	-3467.1	33.4	∼72%
B2V	37.7	14.0	-7.0	-53.1	51.1	∼66%

Table 1: Reduction factor, optimal channeling orientation, bending angle and multiturn channeling efficiency calculated from measurements for all four crystals, both at injection and at flat top energy.

3 Angular scans

Angular scans were performed for all crystals both at injection and at flat top. The optimal channeling orientation and reduction factor were measured for all four of them and are reported in Tab. 1. Fig. 2 and 3 show the angular scans of all crystals at injection and flat top respectively. It is important to keep in mind that the optimal channeling orientation can change between MDs if the goniometer require a reset and lose their reference orientation. Although a recovery procedure has been established, the optimal orientation can change of up to tens of μrad as a result. However, since no reboot of the goniometers were performed since the last measurements, all values are compatible with previous observations [4].

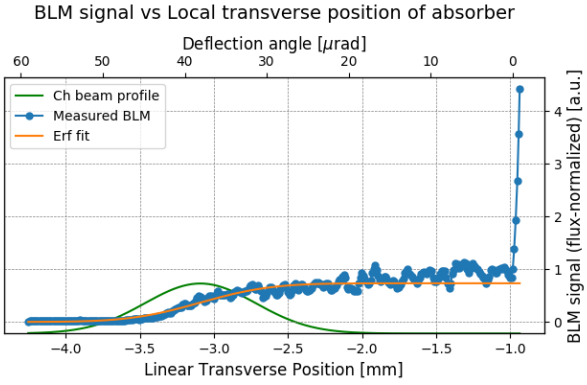

(a) B1V

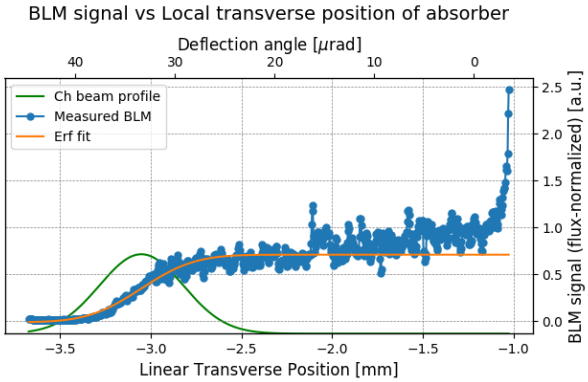

(b) B2H

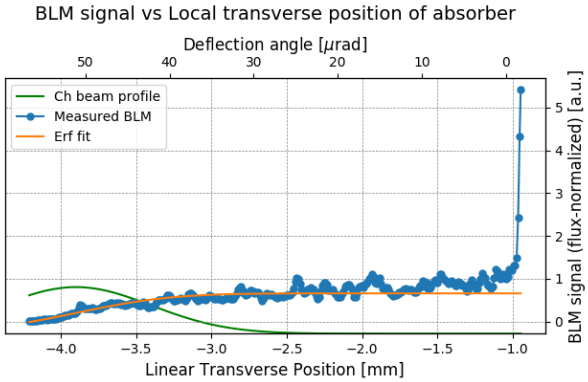

(c) B2V

Figure 4: Linear scans at flat top energy. The BLM signal has been normalized to the particle flux and fitted with an error function to derive the bending angle of each crystal.

4 Linear Scans

Due to time constraints, linear scans were performed only at flat top and with all crystals except B1H, which was already fully characterized in previous MDs [4]. Fig. 4 shows the scans and the measured bending angle are reported in Tab. 1.

The results for the vertical crystals are consistent with previous measurements. Once again, the horizontal crystal on Beam 2 shows a small bending angle at injection, which becomes even smaller at flat top. These results are supported by comparisons of the angular scan with simulations, shown in Fig. 5. This behaviour was already observed in earlier MDs [4] and it is not yet completely understood. It could be linked to the high miscut angle of this crystal, but this needs to be reproduced in simulations to provide a definitive answer.

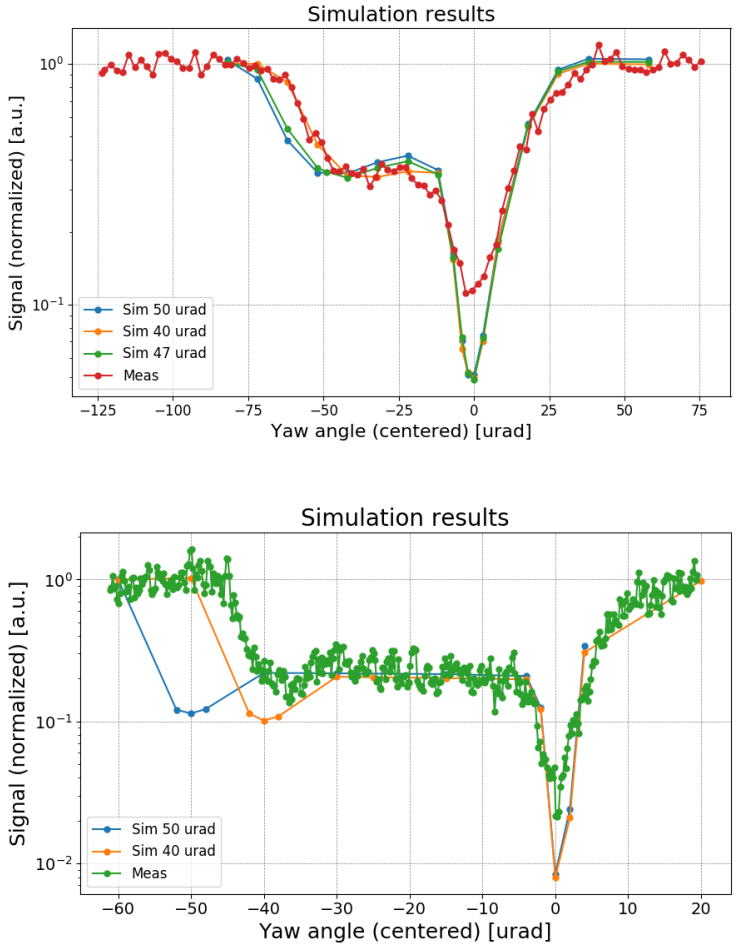

Figure 5: Comparison of B2H angular scan at injection (left) and flat top (right) with simulations with different bending angles.

5 Loss Maps at Flat Top Energy

A series of loss maps were performed at flat top energy with different collimator settings on both beams and planes. In particular, the TCLAs in IR7 were set to progressively tighter apertures (i.e. nominal, 8 σ and 6.5 σ respectively). However, Beam 2 was dumped while loss maps with the last settings were being performed, so only the first two steps are reported for this beam. As in previous MD analysis [3,4,7], the cold region in IR7 is divided into three areas identified by the quadrupoles they include, and the ratio between the losses measured with the standard and crystal-assisted collimation system is calculated for each of them. A ratio larger than 1 indicates an improvement of the cleaning inefficiency when crystals are deployed.

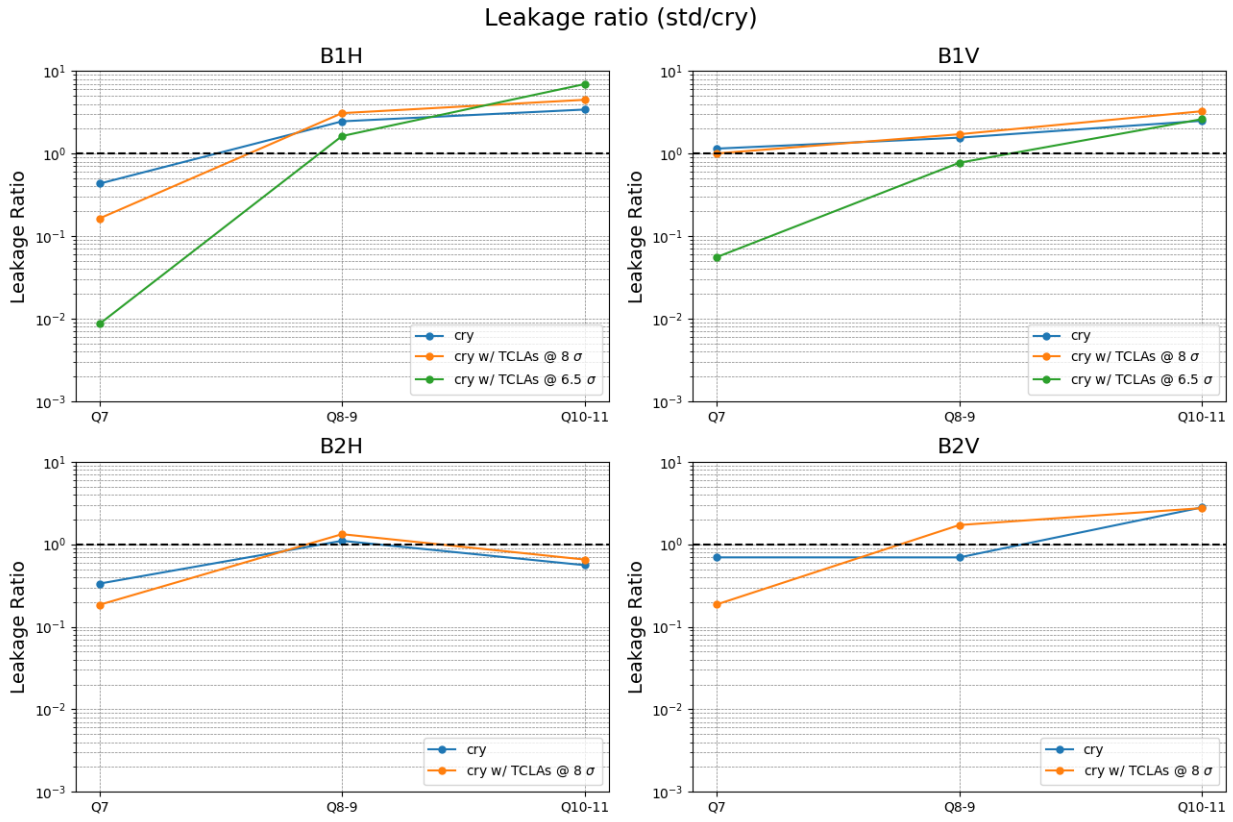

Figure 6: Ratio between losses measured with standard and crystal-assisted collimation system for each IR7 area.

The results are shown in Fig. 6. Beam 1 shows a factor 2-3 improvement in cleaning when crystals are deployed, while results for Beam 2 are less conclusive. It is important to keep in mind that these results are not directly comparable to previous observations since the cleaning of the standard system changed over the years. In particular, the B1V crystal shows lower cleaning ratios than previous measurements [3], and it seems to be less effective than B1H. However, the absolute values of the normalized cleaning inefficiency in Fig. 7 are actually lower for B1V, indicating a better performance than B1H. On the other hand,

the cleaning inefficiency of the standard system, which is a factor 3-4 better for B1V with respect to B1H, which is the main reason why the leakage ratio ends up being lower.

With regards to the worse cleaning in Q7, the current working hypothesis attributes it to showers from upstream collimators. Simulation studies to confirm this hypothesis are currently on-going.

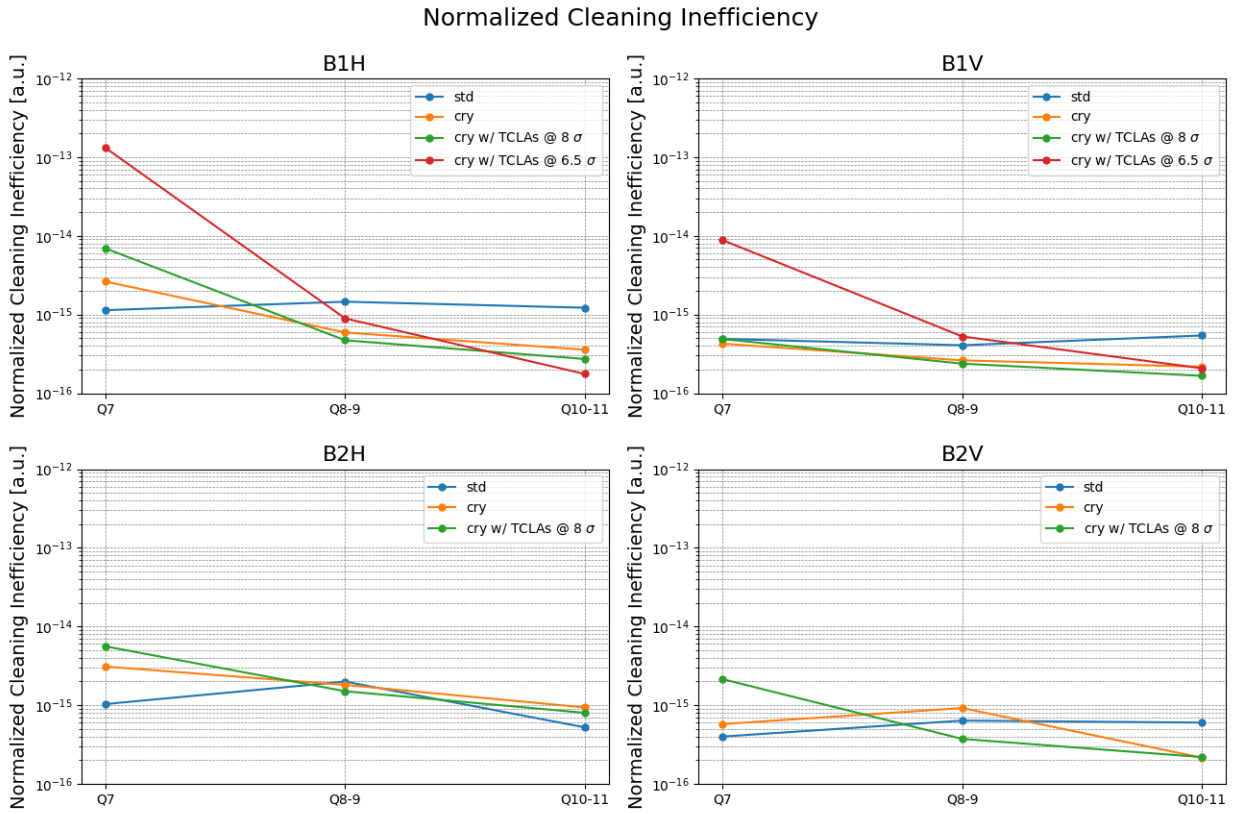

Figure 7: Normalized cleaning inefficiency with standard and crystal-assisted collimation system for each IR7 area.

6 Crystal Channeling during Energy Ramp

Standard collimators are able to follow the adiabatic dumping of the LHC beam during the energy ramp. Crystal devices can be compared to a single sided collimator during beam based alignment. For this reason, the standard collimator ramp functions can be adapted and applied to the linear and rotational stage of the crystals using the same approach [2]:

$$x(t) = x_{CH} - \left[n_{inj} + \frac{n_{ft} - n_{inj}}{\gamma_{ft} - \gamma inj}(\gamma(t) - \gamma_{inj})\right] \times \left[\tilde{\sigma}_{inj} + \frac{\tilde{\sigma}_{ft} - \tilde{\sigma}_{inj}}{\gamma_{ft} - \gamma inj}(\gamma(t) - \gamma_{inj})\right] \frac{1}{\sqrt{\gamma(t)}} \quad (1)$$

$$x'(t) = x'_{CH} - \left[n_{inj} + \frac{n_{ft} - n_{inj}}{\gamma_{ft} - \gamma inj}(\gamma(t) - \gamma_{inj})\right] \times \left[\tilde{\sigma}'_{inj} + \frac{\tilde{\sigma}'_{ft} - \tilde{\sigma}'_{inj}}{\gamma_{ft} - \gamma inj}(\gamma(t) - \gamma_{inj})\right] \frac{1}{\sqrt{\gamma(t)}} \quad (2)$$

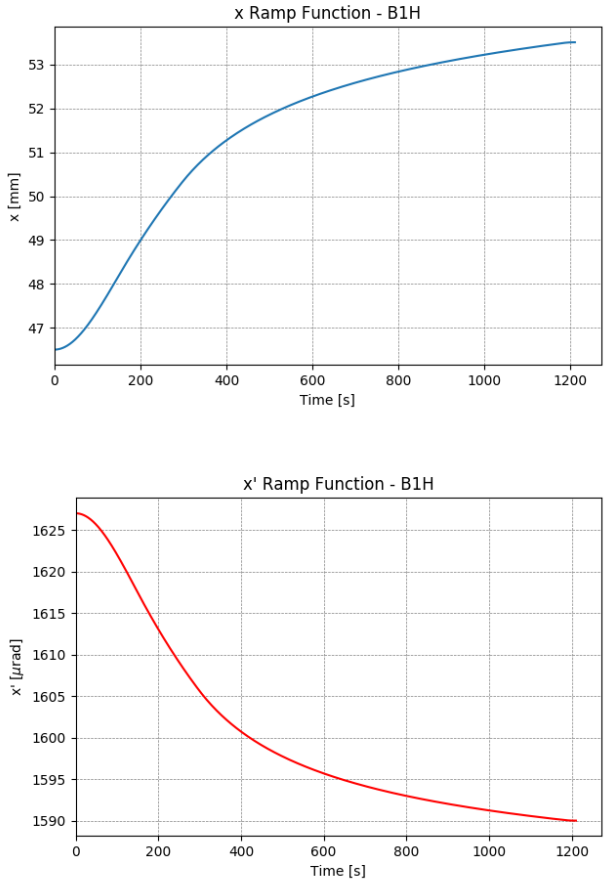

Figure 8: Linear (top) and rotational (bottom) ramp function generated for B1H. The parameters of the functions are adjusted in order to match the beginning and ending positions previously measured.

where n represents the settings in units of sigma, while $\tilde{\sigma}$ and $\tilde{\sigma}'$ are the normalized beam size and divergence respectively. The parameters of Eq. 1 and 2 are adjusted in order to match the beginning and ending points to the values found during the beam base alignment for the linear stage and during the angular scan for the rotational stage. Fig. 8 shows the functions generated for B1H as an example.

Channeling conditions are assessed throughout the ramp by means of continuous loss maps. When crystal-assisted collimation is in place and the crystal is in channeling orientation, losses at the crystal position are lower due to the reduction of nuclear interactions, while losses at the first collimator used as absorber increase. For this reason, the loss pattern in IR7 is different when the crystal is in channeling and amorphous conditions, as shown in Fig. 9. The ratio between losses at the crystal and the absorber can be used as a figure of merit. A ratio above 10^{-2} indicates that channeling conditions are lost [2].

Loss maps were performed roughly every 500 GeV to evaluate the ratio throughout the ramp. The results are shown in Fig. 10. As previously mentioned, there was a trip of the orbit correctors about halfway through the ramp that made measurements performed after this point unreliable. However, the ratio stays under 10^{-2} during the first half, indicating

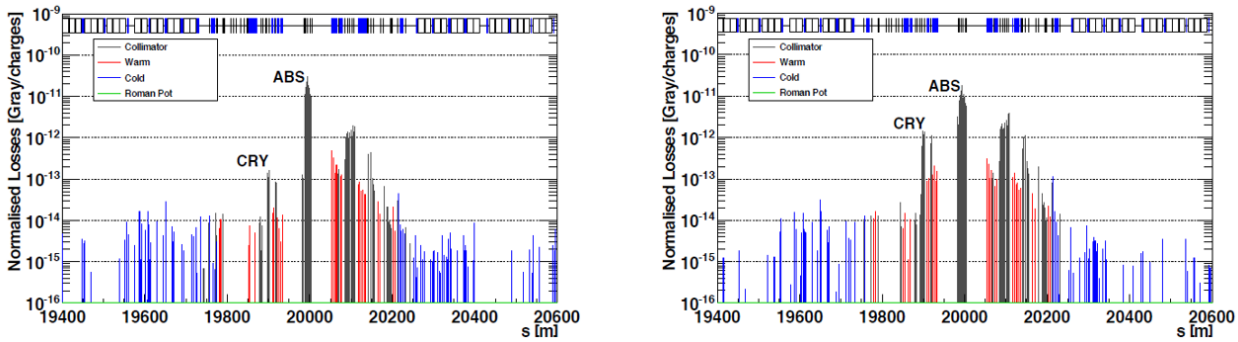

Figure 9: Loss pattern in IR7 during an angular scan when the crystal is oriented in channeling (left) and in amorphous (right). Losses are normalized to the beam flux. Crystal (CRY) and absorber (ABS) are shown on the plots [2].

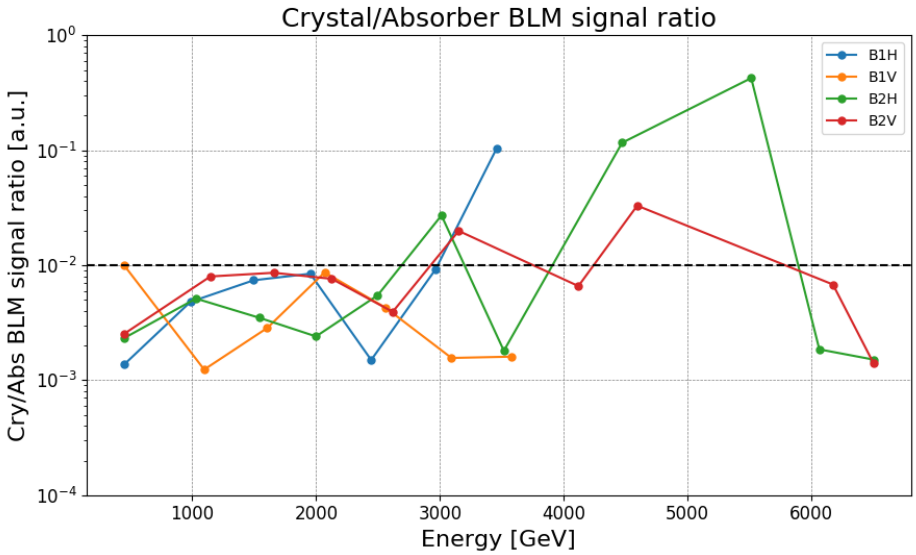

Figure 10: Ratio between losses at each crystal and at the corresponding absorber measured during the energy ramp.

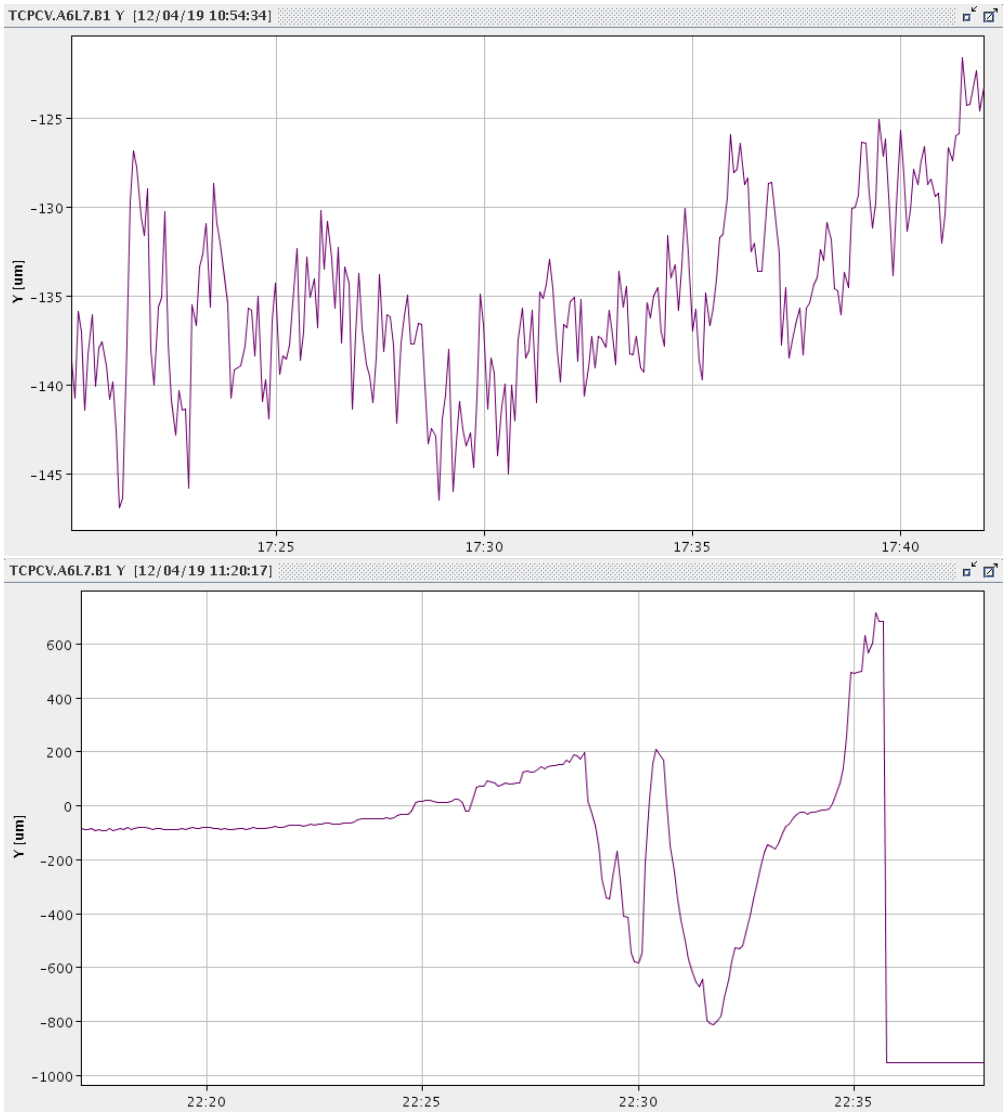

Figure 11: Measured beam position at the B1V crystal location during the ramp without (top) and with (bottom) crystals deployed. The position is calculated as an interpolation of the readouts given by the Beam Position Monitors (BPMs) upstream and downstream the crystal.

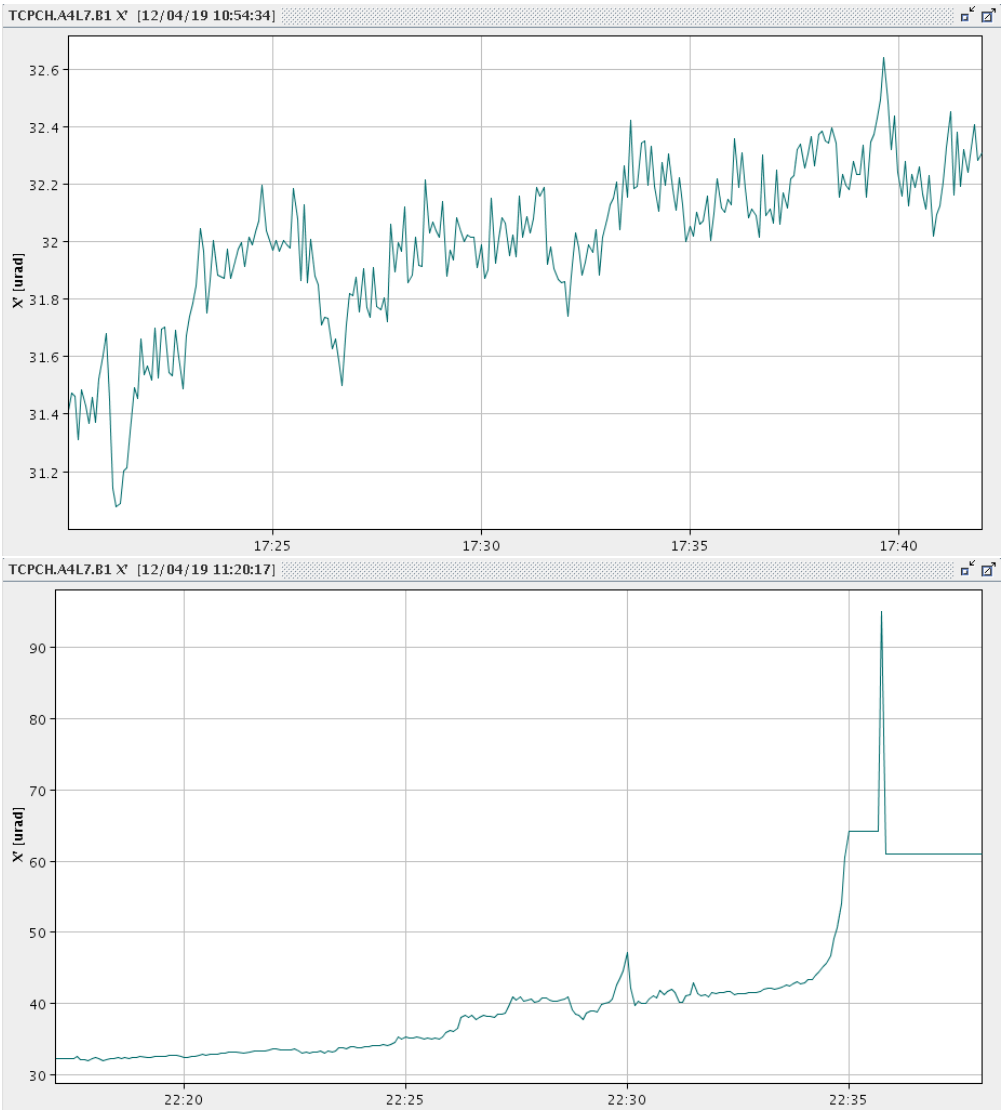

Figure 12: Measured beam angle at the B1H crystal location during the ramp without (top) and with (bottom) crystals deployed. The position is calculated as an interpolation of the readouts given by the Beam Position Monitors (BPMs) upstream and downstream the crystal.

that channeling conditions were kept.

An ideal system with 8 crystals (four per beam and two per plane) would help with dealing with issues regarding the orbit. This is especially true if the beam drifts away from the currently installed crystals towards the other side of the pipe, where no device is present at the moment. During this MD, this situation applied to the vertical plane, where a drift of the orbit towards the inner part of the beam was recorded as shown in Fig. 11 for the vertical crystal on Beam 1 as an example. A second crystal would be able to still catch the drifting beam, allowing to maintain channeling conditions. However, during the trip of the orbit correctors and the subsequent attempts at recovering the orbit, a change in the direction of the orbit at the location of the crystals of some μrad was recorded, as shown in Fig. 12 for B1H as an example. The channeling acceptance depends on the critical angle, which becomes smaller and smaller as the energy increases. Thus, channeling conditions would be lost anyways because the impact angle of the beam would grow out of the acceptance. However, it is important to keep in mind that the machine would be efficiently protected by the interlock system in case an event like this happens.

7 Acknowledgements

We would like to thank the OP crew for their assistance during the MD.

8 References

[1] D. Mirarchi, G. Hall, S. Redaelli, and W. Scandale, "Design and implementation of a crystal collimation test stand at the Large Hadron Collider," *The European Physical Journal C*, vol. 77, no. 6, p. 424, 2017.

[2] R. Rossi *et al.*, "Crystal collimation during the LHC energy ramp." CERN-ACC-NOTE-2018-0053.

[3] R. Rossi, *Experimental assessment of crystal collimation at the Large Hadron Collider*. PhD thesis, Università degli Studi di Roma "La Sapienza", 2017.

[4] M. D'Andrea *et al.*, "Crystal collimation tests with proton beams." CERN-ACC-NOTE-2019-0022.

[5] R. Rossi *et al.*, "Crystal collimation with protons at injection energy." CERN-ACC-NOTE-2016-0035.

[6] R. Rossi *et al.*, "Crystal collimation with protons at flat top energy." CERN-ACC-NOTE-2017-0021.

[7] R. Rossi *et al.*, "Crystal collimation cleaning measurements with proton beams in LHC." CERN-ACC-NOTE-2018-0024.

[8] R. Rossi *et al.*, "Beam 2 crystal characterization measurements with proton beams in the LHC." CERN-ACC-NOTE-2018-0067.